Science of the Total Environment 905 (2023) 167196

Contents lists available at ScienceDirect

Science of the Total Environment

journal homepage: www.elsevier.com/locate/scitotenv

A probabilistic approach to stormwater runoff control through permeable pavements beneath urban trees

Anita Raimondi *, Giacomo Marrazzo, Umberto Sanfilippo, Gianfranco Becciu

Department of Civil and Environmental Engineering, Politecnico di Milano, P.zza L. da Vinci 32, 20133 Milano, Italy

HIGHLIGHTS

- Developed equations can be used to estimate the average runoff and its probability.
- The study examines the influence of the model parameters on the results.
- The analysis considers the pre-filling of the storage volume from previous events.
- System performance depends closely on the infiltration rate into the soil.
- The thickness of the storage layer influences the probability of runoff.

GRAPHICAL ABSTRACT

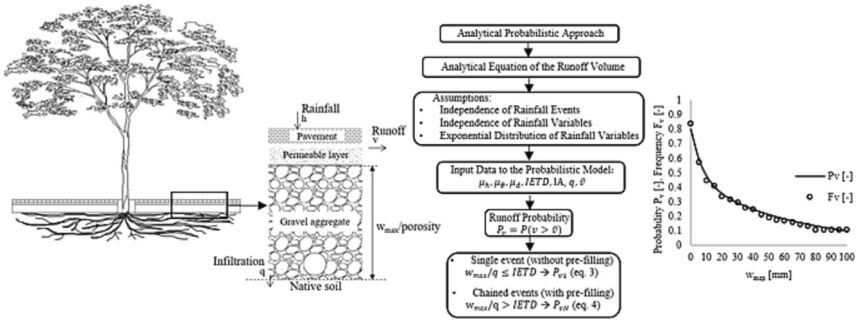

ARTICLE INFO

Editor: Ashantha Goonetilleke

Keywords:
Nature-based solutions
Urban trees
Analytical probabilistic approach
Permeable pavements
Runoff control
Stormwater management

ABSTRACT

One of the most current and urgent challenges is making cities sustainable and resilient to climate change. From this perspective, Nature-Based Solutions (NBSs) are well-recognized strategies for stormwater control and water cycle restoration. Urban trees are an example of NBS. However, the high degree of soil sealing typically found in urban environments limits natural processes such as infiltration and hinders the water and nutrient supply for proper root development, which weakens tree stability. Permeable pavements at the base of urban trees, on the one hand, facilitate infiltration, which helps runoff control, and on the other hand, improve stormwater retention and soil humidity, which enhance root feeding.

This paper proposes an analytical-probabilistic approach to estimate the contribution of permeable pavements to stormwater management. The equations developed in this study relate the runoff probability to the storage volume, the infiltration rate into the underlying soil, and the average values of the hydrological variables in the input. The model allows us to select different runoff thresholds and considers the possibility that residual volume from previous rainfall events prefills the storage capacity.

An application to a case study in Sao Paulo (Brazil) has been presented. It investigates the influence of the different parameters used in the model on the results. The comparison of the outcomes obtained using the developed equations with those obtained from the continuous simulation of measured data confirmed the effectiveness of the proposed analytical-probabilistic approach and the suitability of using permeable pavements at the base of urban trees for improving stormwater retention.

* Corresponding author.
E-mail addresses: anita.raimondi@polimi.it (A. Raimondi), giacomo.marrazzo@polimi.it (G. Marrazzo), umberto.sanfilippo@polimi.it (U. Sanfilippo), gianfranco.becciu@polimi.it (G. Becciu).

https://doi.org/10.1016/j.scitotenv.2023.167196
Received 9 May 2023; Received in revised form 15 September 2023; Accepted 16 September 2023
Available online 21 September 2023

Acronyms and symbols[1]

SDGs	Sustainable Development Goals
NBS	Nature-Based Solution
GI	Green Infrastructures
SUDS	Sustainable Urban Drainage Systems
LID	Low Impact Development
IETD	Inter Event Time Definition
PDF	Probability Density Functions
i	position index of the generic rainfall in the continuous series of events
w_i	water content in the storage volume at the end of the generic rainfall event*[1]
w_{max}	storage volume of the gravel aggregate*
p	porosity of the gravel aggregate
h_{max}	thickness of the gravel aggregate
v_i	runoff at the end of the generic rainfall event
$\bar{v}$	runoff threshold
q	infiltration rate
N	number of chained rainfall events
IA	Initial Abstraction
h	rainfall depth
d	interevent time
θ	rainfall duration
μ_θ	average rainfall event duration
μ_h	average rainfall event depth
μ_d	average interevent time
σ_h	standard deviation of rainfall depth
σ_d	standard deviation of interevent time
σ_θ	standard deviation of rainfall duration
V_h	coefficient of variation of rainfall depth
V_d	coefficient of variation of interevent time
V_θ	coefficient of variation of rainfall duration
$\rho_{h,\theta}$	correlation index between rainfall depth and duration
$\rho_{h,d}$	correlation index between rainfall depth and interevent time
$\rho_{d,\theta}$	correlation index between interevent time and rainfall duration
X	number of rainfall events
E	expected number of events exceeding the runoff threshold
v_{TOT}	total runoff volume*
v_m	average runoff volume*
$p(v)$	runoff probability density function
$P(v)$	runoff cumulative distribution function
r	area ratio
A	catchment area
A_I	infiltration area
φ	runoff coefficient
T	return period
η	performance of the system on stormwater runoff control

1. Introduction

Urban areas must adapt to the critical issues posed by climate change, population growth, and a lack of sustainability. These include water supply during drought periods, stress on drainage systems during heavy rainfall, and the vulnerability of water resources to pollution. Sustainable stormwater management and control and environmental protection are among the seventeen Sustainable Development Goals (SDGs) of the United Nations Agenda 2030 (Goal 6, "Clean water and sanitation", Goal 11, "Sustainable cities and communities", and Goal 13, "Climate action"). The International Union for Conservation of Nature (IUCN) points to NBSs as the leading solutions since their actions, inspired by nature and supported by modern technologies, promote environmental, social, and economic benefits to build resilient systems. Urban trees are an effective NBS, providing several advantages such as heat island reduction, noise and pollution control, biodiversity increase, and landscape improvement (Livesley and McPherson, 2016; Nowak et al., 2014). For example, New York has promoted the "1 million Tree Initiative" (Campbell, 2014); Beijing realized peri-urban parks for a surface equal to 90 times the Olympic Village (Yao et al., 2019); and London aims to reduce the PM10 concentration by about 10 % through urban green areas (Tiwary et al., 2009). Moreover, urban trees facilitate stormwater runoff control and water cycle restoration (Berland et al., 2017; Ruangpan et al., 2020). These beneficial effects are well-known and studied in the literature (Alivio and Bezak, 2023; Konijnendijk et al., 2006). Tree leaves, branches, and trunk surfaces provide interception; their contribution varies sharply within species, tree size, leaf area, leaf smoothness, and bark thickness and roughness (Xiao and McPherson, 2016; Van Stan et al., 2015; Xiao et al., 2000). Roots withdraw water from the soil, which is then released through transpiration by the pores or stomata on the leaf surface. Their growth and decomposition processes also increase the soil infiltration capacity and rate, thus facilitating preferential flow and aquifer recharge (Bartens et al., 2008; Alivio and Bezak, 2023). Despite these recognized benefits, urban trees can be a source of risk due to unstable root anchoring; the soil sealing, typical of the urban environment, limits water and nutrient supply, preventing proper root development (Blunt, 2008). Another critical issue about urban trees is street pavement damage when tree roots raise in search of humidity (Brady and Weil, 2014; Barone and Ferreira, 2019).

The use of permeable pavements at the base of urban trees increases stormwater infiltration, thus helping root development and control of runoff (Mullaney et al., 2015; Ishimatsu et al., 2017). They provide stormwater storage, positively influence soil humidity, and favor groundwater recharge (Scholz and Uzomah, 2013; Johnson, 2015). Permeable pavements are among the most used Low Impact Development (LID) systems since they are part of the street furniture, such as sidewalks, etc., and do not require any additional space (Wang et al., 2019). The positive effect of permeable pavements at the base of urban trees has been well documented by many authors in the literature. Mullaney et al. (2015) concluded that the underlying base layers are essential for tree growth when permeable pavements are on poorly draining soils, as they positively affect soil moisture and temperature and leaf nutrients status. Results of a study by Fini et al. (2017) highlighted that all types of pavements altered the water cycle compared to unpaved soil and that the beneficial effects also depended on the planted species. Morgenroth and Visser (2011) found that porous pavements increased stem height, diameter, and biomass due to their permeability to air and water. Results of experimental measurements by Volder et al. (2009) underlined that lots treated with permeable concrete had higher soil water content than lots with standard concrete in the deeper soil layers in some seasons. Lucke et al. (2011) and Lucke and Beecham (2019) quantified the long-term performance of permeable pavements in reducing stormwater flows and pollution loads, reducing the incidence of structural damage to pavements by tree roots, and favouring healthier and faster-growing trees under typical Australian conditions. They concluded that gravel layers encouraged tree roots to travel deeper into the underlying subgrade soil, and this positive effect increases as the layer thickness increases. A study by Medina Camarena et al. (2022) highlighted that runoff control provided by permeable pavements varies according to soil compaction, infiltration rate, soil type, and system configuration. To maximize the performance of the system, regular maintenance must be provided to ensure full storage capacity and avoid clogging (Winston et al., 2016).

The design of permeable pavements is often based on standard procedures or simplified methods (Weiss et al., 2019). Several methods have been proposed in the literature to model runoff from permeable pavements, among them the Curve Number Method (Leming et al.,

[1] *Volumes are intended for unit of area (water depth).

2007; Madrazo-Uribeetxebarria et al., 2022), numerical models (Eck et al., 2011; Huang et al., 2015), simulation models (Zhang and Guo, 2015; Arjenaki et al., 2021), and experimental studies (Alsubih et al., 2017).

This paper investigates the reduction of stormwater runoff provided using permeable pavements by an analytical-probabilistic approach. The developed equations relate the probability of runoff to the retention volume provided by the permeable pavement, the hydrological input variables, and the infiltration rate into the underlying soil. The method combines the ease of implementation of design storm methods with the reliability of continuous simulation, with no need for long series of recorded data. The analytical-probabilistic approach for the modeling of urban drainage systems was first proposed in the 1990s (Adams and Papa, 2000; Guo and Adams, 1998). In recent years, it has been applied to Sustainable Urban Drainage Systems (Raimondi et al., 2022; Aldrees and Danazumi, 2023), such as green roofs (Zhang and Guo, 2013; Raimondi and Becciu, 2021; Raimondi et al., 2021), permeable pavements (Guo et al., 2018; Cao et al., 2023b), and rainwater harvesting systems (Becciu et al., 2018; Di Chiano et al., 2023). This enabled testing the method under different climatic regimes and outflow rate scenarios.

Very often, most of the analytical-probabilistic approaches presented in the literature consider only partially the possibility of residual volume from previous events pre-filling the storage capacity or even neglect this possibility (Guo and Adams, 1998; Chen and Barry, 2007). When a low outflow rate occurs, as in the case of NBSs, discharged by slow-release processes such as infiltration and/or evapotranspiration, the pre-filling of the retention volume can be due to a chain of previous N rainfall events.

The equations developed in this study keep into account the possibility of pre-filling from previous rainfall events, allow the setting of a runoff threshold to estimate the exceeding probability, and incorporate in the formulation the stormwater runoff from contributing areas. They enable the estimation of the average and cumulative runoff volumes over a chosen period and the evaluation of the performance of the system. Some existing analytical probabilistic models present some of these functions, but in this case, they are combined and included in a comprehensive formulation, making the assessment of the permeable pavement performance more complete. The proposed equations can be used to assess the performance of permeable pavements on stormwater runoff control and the influence of the main parameters influencing the process. They can also be used for the design to identify the required thickness of the gravel aggregate once an acceptable probability of runoff and the porosity of the filling material have been defined. The application to a case study in Sao Paulo (Brazil) and the comparison of results obtained by the application of the developed equations with those obtained by the continuous simulation using a series of recorded data has confirmed that the proposed method is robust and accurate for the modeling of the runoff from permeable pavements.

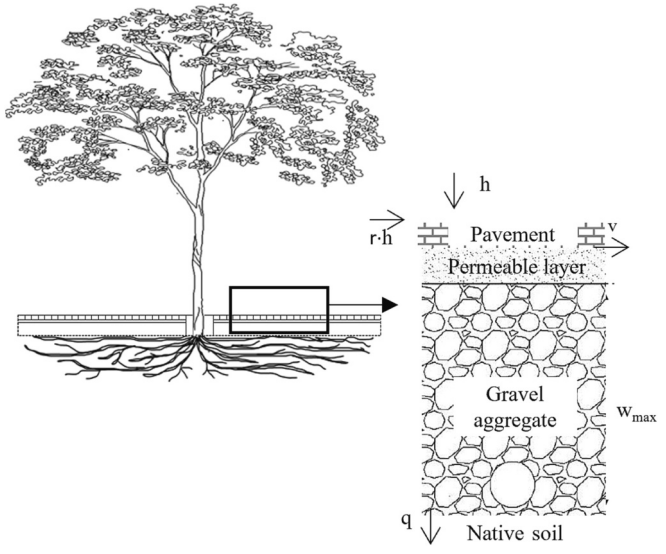

Fig. 1. Permeable pavement integrated at the base of an urban tree; focus on the main layers (h: rainfall depth; v: runoff; q: infiltration rate; w_{max}: storage volume of the gravel aggregate layer).

2. Material and methods

A scheme of permeable pavement integrated at the base of an urban tree was presented in Fig. 1.

The main layers composing a permeable pavement are the surface paving, the permeable layer, and the gravel aggregate. Since the goal of this paper is the probabilistic estimation of stormwater runoff control, the focus is on the gravel aggregate, which is the layer that provides the retention capacity (Marchioni et al., 2021; Leming et al., 2007; Smith, 2011). The thickness of the gravel aggregate (h_{max}) to ensure a storage volume is linked to the porosity (p) of the material constituting the layer by the following relation:

$$w_{max} = h_{max} \bullet p \tag{1}$$

The stormwater retained by the surface paving is then evaporated; the model enables us to consider this component as an Initial Abstraction (IA). The influence of the groundwater table has been neglected; this is because the water balance refers to the first 1–2 m below the ground level, and when considering infiltration, the minimum aquifer level should be at least 1 m below the deeper layer of the system. The assumption is suitable for permeable pavements below urban trees since, in the soil profile, 90–99 % of the total root length is in the upper 1 m of soil (Gasson and Cutler, 1990).

Depending on the infiltration rate into the underlying soil the infiltration can be full or partial (Muttuvelu and Kjems, 2021). In Fig. 1, the case of full infiltration was considered. In the case study, different values of the parameter will be considered to evaluate the suitability of this solution.

To estimate the probability of runoff from permeable pavements at the base of urban trees, the analytical equation of the runoff volume at the end of a generic rainfall event (v_i) was at first defined:

$$v_i = \begin{cases} w_{i-1} - q \bullet d_{i-1} + h_i + r{\cdot}h_i - IA - q \bullet \theta_i - w_{max} & Case\ 1 \\ h_i + r{\cdot}h_i - IA - q \bullet \theta_i - w_{max} & Case\ 2; Case\ 3 \\ h_i + r{\cdot}h_i - IA - q \bullet d_{i-1} - q \bullet \theta_i & Case\ 4 \\ 0 & Otherwise \end{cases} \tag{2}$$

$$Case\ 1: w_{i-1} \le w_{max}; w_{i-1} > q \bullet d_{i-1}; w_{i-1} - q \bullet d_{i-1} + h_i + r{\cdot}h_i - IA - q \bullet \theta_i > w_{max}$$

$$Case\ 2: w_{i-1} \le w_{max}; w_{i-1} \le q \bullet d_{i-1}; h_i + r{\cdot}h_i - IA - q \bullet \theta_i > w_{max}$$

$$Case\ 3: w_{i-1} > w_{max}; w_{max} \le q \bullet d_{i-1}; h_i + r{\cdot}h_i - IA - q \bullet \theta_i > w_{max}$$

$$Case\ 4: w_{i-1} > w_{max}; w_{max} > q \bullet d_{i-1}; w_{max} - q \bullet d_{i-1} + h_i + r{\cdot}h_i - IA - q \bullet \theta_i > w_{max}$$

In Eq. (2), the subscript i is the position index of a generic event in the series, w_{i-1} is the water volume stored at the end of a generic event i-1, d_{i-1} is the dry time between the event i-1 and the event i, θ_i is the rainfall duration of the event i, and r is the ratio between the catchment area A and the infiltration area A_I ($r = A/A_I$).

Case 1 is the condition of no overflow by event i-1 and prefilling of the storage capacity at the beginning of event i. *Case 2* is the condition of no overflow by event i-1 and no prefilling of the storage capacity at the beginning of event i. *Case 3* is the condition of overflow by event i-1 and

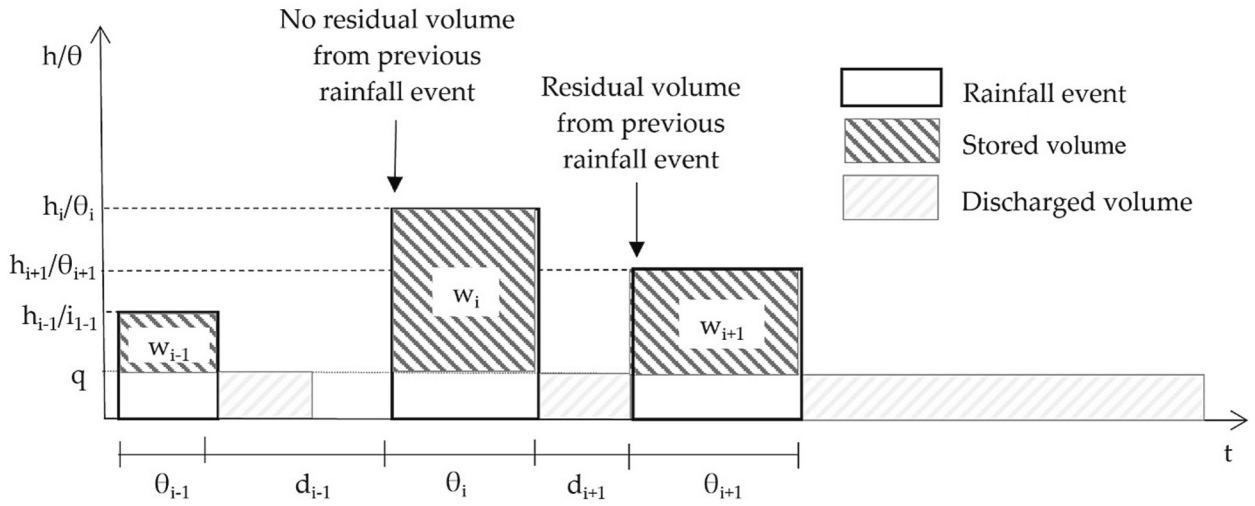

Fig. 2. Consecutive rainfall events without and with prefilling of the storage capacity from previous events.

no prefilling of the storage capacity at the beginning of event *i*. *Case 4* is the condition of overflow by event *i-1* and prefilling of the storage capacity at the beginning of event *i*.

The stormwater volume stored in the permeable pavement at the end of the generic event w_i is:

$$w_i = \begin{cases} w_{i-1} - q \bullet d_{i-1} + h_i + r \cdot h_i - IA - q \bullet \theta_i & Case\ 5 \\ h_i + r \cdot h_i - IA - q \bullet \theta_i & Case\ 6 \\ w_{max} & Case\ 7, Case\ 8 \\ 0 & Otherwise \end{cases} \quad (3)$$

$$Case\ 5: w_{i-1} - q \bullet d_{i-1} > 0; 0 < w_{i-1} - q \bullet d_{i-1} + h_i + r \cdot h_i - IA - q \bullet \theta_i < w_{max}$$

$$Case\ 6: w_{i-1} - q \bullet d_{i-1} \leq 0; 0 < h_i + r \cdot h_i - IA - q \bullet \theta_i < w_{max}$$

$$Case\ 7: w_{i-1} - q \bullet d_{i-1} \leq 0; h_i + r \cdot h_i - IA - q \bullet \theta_i \geq w_{max}$$

$$Case\ 8: w_{i-1} - q \bullet d_{i-1} > 0; w_{i-1} - q \bullet d_{i-1} + h_i + r \cdot h_i - IA - q \bullet \theta_i \geq w_{max}$$

Case 5 is the condition of storage volume prefilling the at the beginning of event *i* and no overflow by event *i*. *Case 6* is the condition of no prefilling of the storage capacity at the beginning of event *i* and no overflow by event *i*. *Case 7* is the condition of no prefilling at the beginning of event *i* and overflow by event *i*. *Case 8* is the condition of prefilling at the beginning of event *i* and overflowing by the end of event *i*. Fig. 2 shows the two scenarios of no residual volume rather than some residual volume remaining from previous rainfall events at the beginning of the next one. In the first case, of course, the time to discharge the stored volume is shorter than the inter-event time. In the second one, the time to discharge the stored volume is longer than the interevent time, and therefore the storage volume is pre-filled from the previous event at the beginning of the new rainfall.

The model considers rectangular rainfall events and constant outflow rates. This last parameter was assumed to be equal to the infiltration rate at saturation in favor of safety when considering runoff from permeable pavements. The model can be applied theoretically at any spatial scale (single building, urban centre, or even large basin). The simplifying assumption of neglecting the effects of peak flow reduction due to catchment routing is suitable for small contribution areas, characterized by negligible concentration time. The hypothesis can be cautiously extended to larger catchments, involving an overestimation of the storage volume. In this study, the catchment is the area of permeable pavement at the base of urban trees. The model also includes the contributions of the neighbouring areas. The terrain slope has not been considered since it is negligible in the slow or flat areas, which are typical for the installation of permeable pavements.

From the continuous chain of rainfalls, independent events were identified by the definition of a Minimum InterEvent Time (MIET), often called Inter Event Time Definition (IETD) in literature; if the interevent time between two consecutive rainfall events was lower than *IETD*, then these two events have been joint. The compound event has depth equal to the sum of the two single depths and a duration equal to the sum of the two durations plus the dry time between the two events. On the contrary, when the interevent time between two consecutive rainfall events was higher than *IETD*, the two events were considered separate.

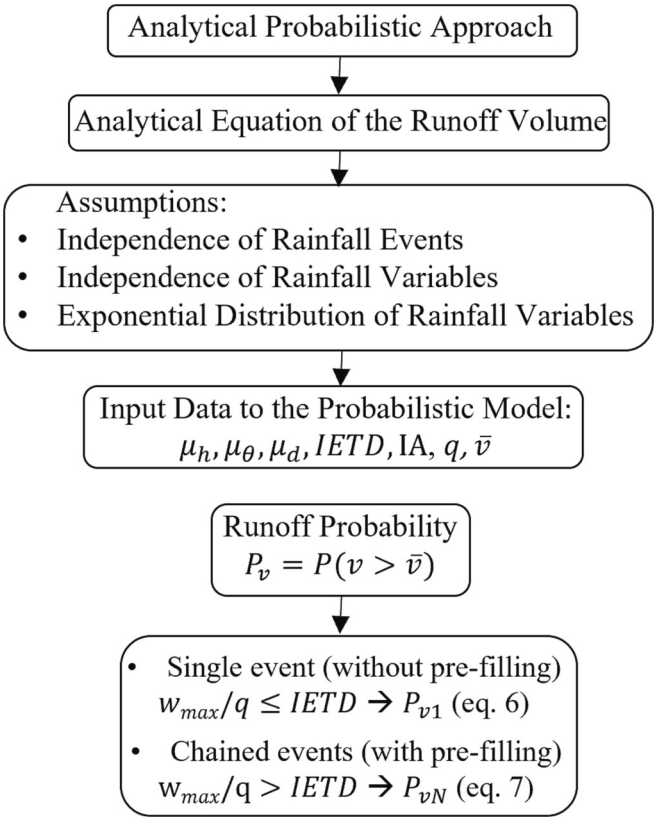

Fig. 3. Flow chart of the analytical probabilistic model developed for the estimation of the runoff probability from permeable pavements.

The input hydrological variables to the model rainfall depth h, rainfall duration θ, and interevent time d, were considered exponentially distributed:

$$f_h = \xi \bullet e^{-\xi \bullet h} \tag{4}$$

$$f_\theta = \lambda \bullet e^{-\lambda \bullet \theta} \tag{5}$$

$$f_h = \psi \bullet e^{-\psi \bullet (d - IETD)} \tag{6}$$

With: $= 1/\mu_\theta$, $\xi = 1/\mu_h$, and $\psi = 1/(\mu_d - IETD)$.

μ_θ, μ_h and μ_d are respectively the average rainfall depth, average duration and interevent time.

Although, depending on the rainfall regime, other PDFs, such as the Weibull, double-exponential, and Gamma, were demonstrated to be suitable for fitting the series of recorded data (Balistrocchi and Bacchi, 2011), this hypothesis proved not to affect the reliability of results (Becciu and Raimondi, 2012). In addition, the exponential PDF is easy to derive and only requires knowledge of the average value of the input variables.

Another assumption of this method is that it considers the hydrological variables independent. While both the correlation between interevent time and rainfall duration and the correlation between interevent time and rainfall depth are often negligible, the correlation between rainfall depth and duration can be significant. In literature, the copula functions overcome this limit by considering bivariate variables (Salvadori and De Michele, 2007; Zhang and Singh, 2007). Previous applications of the analytical-probabilistic approach showed that the assumption of independence among rainfall variables did not influence the goodness of results (Raimondi and Becciu, 2015).

In the modeling, two conditions were distinguished:

- $w_{max}/q \leq IETD$: the time needed to empty the storage volume is lower than *IETD*, so the retention capacity is fully available at the beginning of each rainfall event; the model considers a single event ($N = 1$) isolated from the rainfall series.
- $w_{max}/q > IETD$: the time needed to empty the storage volume is higher than *IETD,* so there is the possibility that the storage volume is partially pre-filled from previous rainfall events ($N > 1$).

This second condition is typical of systems with low outflow rates or/and short interevent time. For $w_{max}/q \leq IETD$, the probability that runoff exceeds a fixed threshold ($\bar{v}$) is:

$$P_{v1} = Prob(v > \bar{v}) = \int_{h=\frac{w_{max}+\bar{v}+IA+q\bullet\theta}{1+r}}^{\infty} f_h dh \bullet \int_{\theta=0}^{\infty} f_\theta \, d\theta = \gamma \bullet e^{-\frac{\xi}{1+r}\bullet(w_{max}+\bar{v}} + IA) \tag{7}$$

with $\gamma = \frac{\lambda \bullet (1+r)}{\lambda \bullet (1+r) + q \bullet \xi}$.

For $w_{max}/q > IETD$, the probability that runoff exceeds a fixed threshold ($\bar{v}$) is:

$$P_{vN} = P(v > \bar{v}) = \int_{h=\frac{q\cdot\theta+IA+w_{max}+\bar{v}}{1+r}}^{\infty} f_h \cdot dh \cdot \int_{\theta=0}^{\infty} f_\theta \cdot d\theta +$$

$$+ \sum_{n=2}^{N} \int_{h=\frac{q\cdot\theta}{1+r}+\frac{w_{max}+IA+(n-2)\cdot q\cdot d}{(n-1)\cdot(1+r)}}^{\frac{q\cdot\theta}{1+r}+\frac{w_{max}+IA+\bar{v}+(n-1)\cdot q\cdot d}{n\cdot(1+r)}} f_h \cdot dh \cdot \int_{d=IETD}^{\frac{w_{max}}{q}} f_d \cdot dd \cdot \int_{\theta=0}^{\infty} f_\theta \cdot d\theta =$$

$$= \gamma \cdot \left\{ e^{-\frac{\xi}{1+r}\cdot(w_{max}+\bar{v}+IA)} + \psi \cdot (1+r) \cdot \sum_{n=2}^{N} \left[-(n-1) \cdot \beta_n^* \cdot \right.\right.$$

$$\left. e^{\frac{\xi}{(n-1)\cdot(1+r)}\cdot[q\cdot IETD\cdot(n-2)+IA+w_{max}+\bar{v}]} - n \cdot \beta_n \cdot \left(e^{-\frac{\xi}{n\cdot(1+r)}\cdot[(n-1)\cdot q\cdot IETD+IA+\bar{v}+w_{max}]} - \xi \cdot q \cdot \beta_n \cdot \beta_n^* \cdot \right.\right.$$

$$\left.\left. e^{\psi\cdot IETD-(w_{max}+\bar{v})\cdot\left(\frac{\psi}{q}+\frac{\xi}{1+r}\right)} \right) \right] \right\} \tag{8}$$

(8)

with $\beta_n = -\frac{1}{q\bullet\xi\bullet(n-1)+n\bullet\psi\bullet(1+r)}$ and $\beta_n^* = \frac{1}{q\bullet\xi\bullet(n-2)+\psi\bullet(n-1)\bullet(1+r)}$.

For $N = 2$, Eq. (8) results:

$$P_{v2} = \gamma \bullet \left\{ \left(1 - \beta_2^{'}\right) \bullet \left[e^{-\frac{\xi}{2\bullet(1+r)}\bullet(q\bullet IETD+\bar{v}} + w_{max} + IA) \right] + \beta_2^{'} \right.$$

$$\left. \bullet\, e^{\psi\bullet IETD-(\bar{v}} + w_{max} + IA) \bullet \left(\frac{\psi}{q} + \frac{\xi}{1+r} \right) \right\} \tag{8'}$$

with $\beta_2^{'} = \frac{\xi\bullet q}{q\bullet\xi+2\bullet\psi\bullet(1+r)}$.

Each term in the sum of Eq. (8) is related to the condition explained by Case 5, Case 6, and Case 7 and Case 8 of Eq. (3). The details of the procedure to derive Eqs. (7) and (8) are presented in the Appendix section.

The runoff threshold $\bar{v}$ enables us to verify if the runoff volume is acceptable for the drainage capacity of the downstream network and to evaluate the potential effects of flooding. Fig. 3 summarizes the flow chart of the main steps of the proposed analytical-probabilistic approach for the estimation of the probability of runoff from permeable pavements. The proposed equations can be used to assess the performance of existing systems or for the design of the retention volume.

If X is the average number of rainfall events occurring in the considered period, the expected number of events E above the fixed threshold can be estimated by:

$$E = X \bullet P(\bar{v}) \tag{9}$$

The mean value of the runoff volume (v_m) is:

$$v_m = \int_{\bar{v}}^{\infty} v \bullet p(v) dv \tag{10}$$

being $p(v) = dP(v)/dv$ the PDF of $P(v)$.

Considering X events, the total runoff volume (v_{TOT}) is:

$$v_{TOT} = X \cdot v_m = X \cdot \int_{\bar{v}}^{\infty} v \bullet p(v) dv \tag{11}$$

The ratio between the runoff and the rainfall depth allows us to evaluate the performance η of the system on stormwater runoff control:

$$\eta = 1 - \frac{v}{h} \tag{12}$$

where η can range between 0 and 1. For η=1 a total stormwater runoff control occurs. Eq. (12) can be used for both a single event and for a series of events during a given period of time.

3. Case study

The proposed approach was applied to the city of Sao Paulo (Brazil). The municipality of Sao Paulo counts 646,310 trees planted along the road system (17,800 km) of its 32 boroughs (Sao Paulo Cidade, 2015). Soil sealing limits stormwater infiltration and prevents proper root feeding and development. The unsteady anchor is one of the main causes of trees falling (Jim, 2017). In the Municipality of Sao Paulo, this issue is of great concern; in the period 2014–2020, 18,194 trees fell and 776 fell in the summer of 2021 alone (Marchioni et al., 2022a, 2022b). Rosa et al. (2018) concluded that between 2016 and 2018 in Sé Subprefecture, 68 % of trees fell for root rupture. Decree number 52.903/12 of Sao Paulo Municipality established that public sidewalks must have a minimum width of 1.20 m free of obstacles for pedestrians. Decree number 49.904/05 established that when present, the service lane intended for urban furniture and vegetation must be at least 70 cm wide. Thus, trees are planted only on sidewalks with a minimum width of 1.90 m. Integrating infiltration systems, such as permeable pavements at the base of urban trees, as alternatives to impervious pavements can improve urban tree well-being and help to control runoff and restore the water cycle. When adequate soil humidity is guaranteed, tree roots can better develop, reducing the risk of falling.

According to Köppen and Geiger (Kottek et al., 2006), the climate in the city of Sao Paulo is classified as CFA (warm and temperate). The average annual rainfall (P) is about 1356 mm, with significant

pluviometry variations throughout the year: the driest month is August, with an average rainfall of 40 mm; the most rainfall concentrates in January, with an average rainfall depth of 228 mm and a mean of 17 rainy days. The average annual temperature (T) is 19.5 °C, with an average temperature of 22.5 °C in February, the warmest month of the year, and an average temperature of 16.2 °C in July, the coldest month. The relative humidity (U) is over 70 %. The lowest measured value is 74.15 % (in August), while the highest is 83.95 % (in March). Table 1 summarizes data about the climate in Sao Paulo in the 1991–2021 period.

The city of Sao Paulo is affected by climate change and suffers increased temperatures. The results of a study by Gozzo et al. (2019) have foreseen an increase in temperature from 1 to 2 °C for the 2010–2030 period, from 2 to 3 °C for the 2040–2050 period, and of 4 °C for the 2080–2090 period. The increase in temperatures is often associated with an increase in high-intensity rainfall events and drought periods (WMO, 2021). Schardong and Srivastav (2014) expected extreme events to increase by >30 % (100-years return periods) in the city of Sao Paulo. In this study, the rainfall data are those provided by the Fundação Centro Tecnológico de Hidráulica recorded at rainfall station number 273 (located at the mouth of the Pirajuçara stream). Data were recorded from May 2007 to October 2017, with a time step of 10 min and a resolution of 0.2 mm.

A monthly scale was used for the analysis. It resulted in the most suitable solution since it allows us to consider the variability of the rainfall and climatic variables (Raimondi et al., 2023). The application focused on January, the rainiest month of the year and therefore the most interesting one in terms of stormwater runoff. The average values of rainfall depth, duration, and interevent time of rainfall events were used as input into the model. To identify independent rainfall events, four values of *IETD* (1–6–12-24 h) were considered in line with the literature (Cao et al., 2023a; Lee and Kim, 2018). Two different values of Initial Abstraction were used in the calculation (IA = 2 mm and IA = 4 mm). They were suitable to ensure the reliability of the analysis and to consider the losses due to the evapotranspiration of stormwater stored in the surface paving (Garofalo et al., 2016).

Table 2 shows the average values of rainfall variables (rainfall depth h, rainfall duration θ, and interevent time d), the mean number of events (X), the coefficients of variation (V), and the correlation indexes between (ρ) for each *IETD*.

In the following, IETD = 24 h, which involved few average rainfall events and was not coherent with the records of the periods considered, was excluded. IETD = 6 h is the most suitable value to satisfy the assumptions of exponential distribution and independence of the input hydrological variables to the model, $V \approx 1$ and $\rho \approx 0$ (see Table 2).

To compare the effectiveness of the permeable pavement with different underlying soils, the analyses considered three values of the infiltration rate: q = 0.036–0.36-3.6 mm/h, corresponding respectively to 10^{-6} m/s (fine sands), 10^{-7} m/s (clayey silts), and 10^{-8} m/s (mixtures of sand, silt, and clay). These values were defined according to the typical range of infiltration rates found in the literature (Terzaghi et al., 1996). The storage volume w_{max} was varied between 0 and 100 mm. This range corresponds to the typical thickness of the gravel aggregate layer used in practice and found in the literature (Weiss et al., 2019). Two runoff thresholds ($\bar{v}$=0 mm and $\bar{v}$=5 mm) were considered in the calculation. The first corresponds to the possibility of runoff and the value of 5 mm, corresponds to the so-called first flush, generally considered by law and regulations (Todeschini et al., 2019).

The proposed approach was used to test the performance of a permeable pavement designed using the "design storm approach", with the following parameters of the depth-duration-frequency curve: a = 61 mm/h^n, n = 0.21, corresponding to a return period T = 10 years (Marchioni et al., 2022a, 2022b):

$$w_{max} = \theta_w \bullet \left(\varphi \bullet a \bullet \theta_w^{n-1} \bullet r - f_c\right) \tag{13}$$

with: $\theta_w = \left(\frac{f_c}{\varphi \bullet a \bullet n \bullet r}\right)^{\frac{1}{n-1}}$; φ is the runoff coefficient (set equal to 1).

The contributing area was neglected in the calculation (r = 0).

The results obtained by the application of Eqs. (7) and (8) were also compared with the frequency probability function estimated by the continuous simulation using the series of recorded data (Eq. (2)). In this study, the analysis was performed using MATLAB. However, it could be performed by other simulation software.

4. Results and discussion

Fig. 4 shows the influence of different values of IETD (1 h, 6 h, and 12 h) on the runoff probability (P_v), for q = 0.036 mm/h (Fig. 4a), q = 0.36 mm/h (Fig. 4b), and q = 3.6 mm/h (Fig. 4c), varying the storage volume w_{max}. The Initial Abstraction and the runoff threshold have been set, respectively, equal to IA = 2 mm and $\bar{v}$ = 0 *mm*.

The probability of runoff is comparable for IETD = 6 h and IETD = 12 h, while it is underestimated for IETD = 1 h. The probability of runoff decreases as the storage volume of the gravel aggregate grows. When the infiltration rate is q = 3.6 mm/h, the runoff probability remains low for the whole range of storage volumes selected in the analysis and becomes negligible for values higher than 40 mm. For an infiltration rate of q = 0.036 mm/h, the runoff probability remains high for all values of storage volume and only slightly decreases as the infiltration rate increases. In this case, it is suitable to equip the permeable pavement with a drainage pipe to avoid flooding and guarantee a suitable emptying time (Marchioni et al., 2022a, 2022b). This can be omitted when the average and total runoff volumes are acceptable for the downstream drainage network. Furthermore, since the sidewalk is not subject to vehicular traffic and one of the aims of integrating permeable pavements at the base of urban trees is to maintain soil humidity, there is no need to check the emptying time (48 h is generally acceptable for infiltration systems, although in Sao Paulo rainfall events are frequent in January). When the infiltration rate is q = 0.36 mm/h, the runoff probability is considerably influenced by the storage volume in the gravel aggregate. It can significantly decrease, increasing the thickness of the gravel aggregate layer (related by the porosity to the storage capacity, see Eq. (1)). The infiltration rate is the parameter that most affects not only the runoff probability but also the number of chained events. For q = 3.6 mm/h, the retention capacity can be empty during the interevent time, and there is no pre-filling of the retention volume from previous rainfall events (N = 1). For q ≈ 0.36 mm/h, the prefilling of the storage capacity is not negligible and must be considered when modeling the runoff probability. In the specific case IETD = 6 h, the number of chained rainfalls is N = 4. For q = 0.036 mm/h the number of chained rainfall events is very high. It means that the storage capacity of the gravel aggregate cannot be emptied after each storm event. In this case, a drainage pipe should be included to limit the risk of flooding.

The results of the same analysis as in Fig. 4, performed considering

Table 1
Average monthly climate variables measured in Sao Paulo in the 1991–2021 period (https://it.climate-data.org).

	Jan	Feb	Mar	Apr	May	Jun	Jul	Aug	Sep	Oct	Nov	Dec
T [°C]	22.3	22.5	21.6	20.2	17.5	16.7	16.2	17.2	18.6	19.8	20.1	21.6
P [mm]	228	167	150	69	64	46	56	40	92	117	152	175
U [%]	83	83	84	82	80	78	76	74	76	80	83	83
N° of rainy days	17	14	15	8	6	4	4	4	8	11	13	15

Table 2
Average values of number of events (X), rainfall depth (μ_h), duration (μ_θ), and interevent time (μ_d), coefficients of variation (V), and correlation indexes (ρ) among rainfall variables for different *IETD*, January (2007–2017).

IETD [h]	X [−]	μ_h [mm]	μ_θ [h]	μ_d [h]	V_h [mm]	V_d [h]	V_θ [h]	$\rho_{h,d}$ [−]	$\rho_{\theta,h}$ [−]	$\rho_{d,\theta}$ [−]
1	17	11.7	4.3	36.2	1.15	1.17	0.76	−0.10	0.44	−0.10
6	14	16.4	11.0	42.9	1.04	1.02	1.06	−0.14	0.62	−0.12
12	11	21.5	20.5	48.0	1.19	0.92	1.06	−0.16	0.74	−0.18
24	6	40.1	57.5	66.3	1.50	0.66	1.14	−0.18	0.90	−0.11

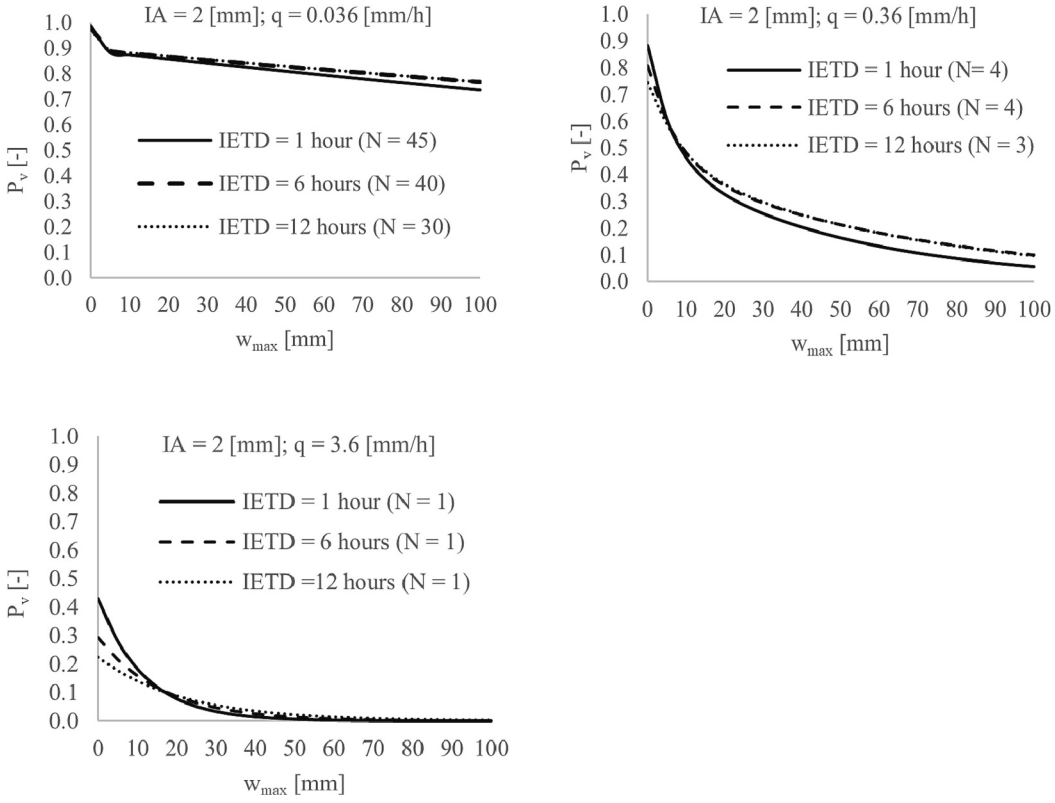

Fig. 4. Probability of runoff (P_v) varying the storage volume of the gravel aggregate (w_{max}) for *IETD = 1–6-12 h and q = 0.036 mm/h (a), q = 0.36 mm/h (b), and* q = 3.6 mm/h (c). IA = 2 mm and $\bar{v}$=0 mm.

IA = 4 mm instead of IA = 2 mm, are presented in the Appendix section (Fig. A1). Fig. A2 (always in the Appendix section) visualizes a comparison between the results obtained considering the two different values of initial abstraction considered in the analysis (IA = 2 mm and IA = 4 mm).

Fig. 5 shows the comparison between the probability of runoff (P_v), obtained by the application of Eqs. (7) and (8), and the runoff frequency (F_v), obtained from the continuous simulation (Eq. (2)) using the series of the observed data. IETD = 6 h, q = 0.36 mm/h, and $\bar{v}$=0 mm (Fig. 5a) and $\bar{v}$= 5 mm (Fig. 5b) have been considered in the analysis. The same analysis, considering q = 0.036 mm/h and q = 0.36 mm/h was reported in the Appendix (Fig. A3).

The number of chained rainfall events has been estimated through the least square method, selecting the best fit between the results

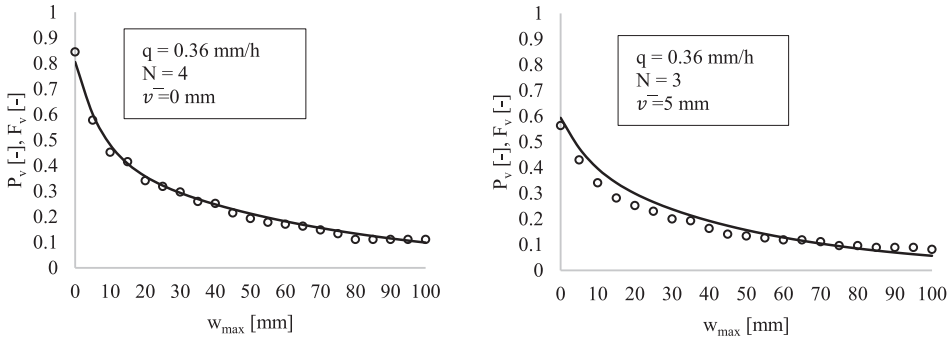

Fig. 5. Runoff probability (P_v) and frequency (F_v) varying the retention volume (w_{max}) of the gravel aggregate, considering two different runoff thresholds $\bar{v}$=0 mm (a) and $\bar{v}$=5 mm (b). For IETD = 6 h, q = 0.36 mm/h, and IA = 2 mm.

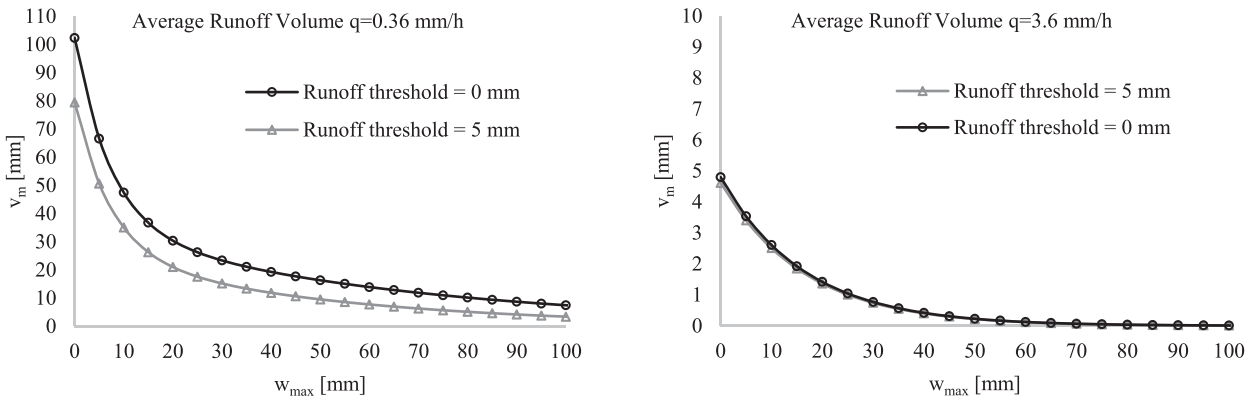

Fig. 6. Average runoff (v_m) varying the storage volume (w_{max}), considering two different runoff thresholds $\bar{v}$=0 mm and $\bar{v}$=5 mm for infiltration rates q = 0.36 mm/h (a) and q = 3.6 mm/h (b). IETD = 6 h.

obtained by the application of the proposed equations and the frequency distribution function of the results obtained by the application of the Eq. (2) using the series of observed data.

When the storage volume is null ($w_{max} = 0$), the runoff probability is higher than 80 %; since the average number of rainfall events (X) recorded in January for the 2007–2017 period is 14, the rainfall events that produced runoff were about 11. The probability reduces to 60 %, considering a runoff volume threshold of 5 mm. In this case, 8 events out of 11 produce runoffs. A permeable pavement with a storage volume of about 50 mm reduces the probability of stormwater runoff to 20 % considering a runoff threshold of 0 mm and to 15 % considering a runoff threshold of 5 mm. This means that in the first case, only 3 events out of 11 produce runoffs, while in the second case, the events producing runoff are only 2 out of 11. This offers a meaningful example of the contribution of permeable pavements to stormwater runoff control.

Fig. 6 shows the average runoff volume (v_m) estimated by Eq. (10) as a function of the storage volume (w_{max}), for the two runoff thresholds considered in the analysis ($\bar{v}$=0 mm and $\bar{v}$=5 mm) for an infiltration rate equal to q = 0.36 mm/h (Fig. 6a) and 3.6 mm/h (Fig. 6b).

Considering an infiltration rate of 3.6 mm/h, the stormwater runoff is null with a storage volume higher than 6 cm (the performance of the systems on the stormwater runoff control is $\eta = 1$), while it is maximum ($v_m = 5$ mm) when the retention storage is null ($\eta = 0.7$). For an infiltration rate of 0.36 mm/h, without retention volume ($w_{max} = 0$ mm), the average runoff volume is higher than 10 cm ($\eta < 0.4$). This value can be greatly reduced by considering permeable pavement. Considering a storage volume of the gravel aggregate equal to $w_{max} = 50$ mm, the average runoff volume falls to 2 cm. This example again highlights the crucial role of permeable pavements in stormwater runoff control. Considering the "design storm approach" (Eq. (13)), the storage volume for a design return period $T = 10$ years and q = 0.036 mm/h, resulted equal to 124 mm; this agrees with the results obtained with the proposed equations. As presented in Fig. 5a, for q = 0.036 mm/h, a probability of runoff $P_v = 0.1$ corresponds to a storage capacity of the gravel aggregate slightly higher than 10 cm.

5. Conclusions

Permeable pavements, integrated at the base of urban trees, help to control stormwater runoff by facilitating infiltration and stormwater retention. The proposed analytical probabilistic model allows us to estimate the probability of runoff from a permeable pavement by relating it to the design variables. The runoff probability strictly depends on the infiltration rate into the underlying soil. For some kinds of soils, infiltration is not suitable, and a drainage pipe must be added; for others, a careful sizing of the storage volume is fundamental to achieving a good level of stormwater runoff control. Comparing the results obtained by the developed equations with those obtained by the continuous simulation of recorded data and the application of the "design storm approach", has confirmed the goodness and accuracy of the method. Taking into account the residual volume from previous rainfall events is fundamental for the reliability of results, since when the infiltration rate is low, the probability of the storage volume pre-filling is not negligible. The proposed method can be helpful for designers to assess the performance of permeable pavements in reducing stormwater runoff in different conditions. It also enables the calculation of the average and total runoff volumes to estimate the risk of flooding from the drainage system. The analytical probabilistic approach can be applied to different climate regimes and soils. It has been applied considering the whole stochastic process (average values of the hydrological variables of all rainfall events in the considered period). Further development will aim to evaluate its suitability using extreme events, and its application to rainfall series considering the climate. The role of NBSs, such as permeable pavements at the base of urban trees, may appear to be limited when the catchment area is small. However, big cities have dozens of thousands of kilometers of roads, and permeable pavements along the tree-lined sidewalks would significantly reduce runoff volumes, considerably helping to manage stormwater. Further analysis will also focus on the evaluation of the combined effects of permeable pavements and urban trees on water cycle restoration, in particular how tree roots improve the infiltration rate into the underlying soil.

CRediT authorship contribution statement

Conceptualization, Anita Raimondi
Methodology, Anita Raimondi and Gianfranco Becciu
Validation, Anita Raimondi, Giacomo Marrazzo
Formal analysis, Anita Raimondi
Data curation, Anita Raimondi, Giacomo Marrazzo
Writing—original draft preparation, Anita Raimondi
Writing review and editing, Anita Raimondi, Giacomo Marrazzo and Umberto Sanfilippo
Supervision, Anita Raimondi
Project administration: Anita Raimondi and Gianfranco Becciu
All authors have read and agreed to the published version of the manuscript.

Declaration of competing interest

The Authors declare that they have no conflict of interest.

Data availability

Data will be made available on request.

Acknowledgments

We would like to thank the Fundação Centro Tecnológico de Hidráulica for providing the rainfall data used in this study.

Appendix A. The procedure to derive Eqs. (7) and (8) is detailed below

For $N = 1$, single rainfall, the runoff at the end of the event is:

$$v_1 = \begin{cases} h_1 + r{\cdot}h_1 - IA - q \bullet \theta_1 - w_{max} & h_1 + r{\cdot}h_1 - IA - q \bullet \theta_1 > w_{max} \\ 0 & Otherwise \end{cases}$$

The condition $v_1 > \bar{v}$ results: $h_1 + r{\cdot}h_1 - IA - q \bullet \theta_1 - w_{max} > \bar{v}$, that is: $h_1 > \frac{IA + q \bullet \theta_1 + w_{max} + \bar{v}}{1+r}$.

Assuming, $h = h_1$ and $\theta = \theta_1$, the probability that runoff exceeds the selected threshold is:

$$P_{v1} = Prob(v > \bar{v}) = \int_{h=\frac{w_{max}+\bar{v}+IA+q\bullet\theta}{1+r}}^{\infty} f_h dh \bullet \int_{\theta=0}^{\infty} f_\theta \, d\theta = \gamma \bullet e^{-\frac{\xi}{1+r}\bullet(w_{max}+\bar{v})}$$

For $N = 2$, a couple of events, the runoff at the end of the second rainfall is:

$$v_2 = \begin{cases} h_1 + r{\cdot}h_1 - IA - q \bullet \theta_1 - q \bullet d_1 + h_2 + r{\cdot}h_2 - IA - q \bullet \theta_2 - w_{max} & Case\ 1 \\ h_2 + r{\cdot}h_2 - IA - q \bullet \theta_2 - w_{max} & Case\ 2; Case\ 3 \\ h_2 + r{\cdot}h_2 - IA - q \bullet d_1 - q \bullet \theta_2 & Case\ 4 \\ 0 & Otherwise \end{cases}$$

$$Case\ 1 : h_1 + r{\cdot}h_1 - IA - q \bullet \theta_1 \le w_{max}; h_1 + r{\cdot}h_1 - IA - q \bullet \theta_1 - q \bullet d_1 > 0; h_1 + r{\cdot}h_1 - IA - q \bullet \theta_1 - q \bullet d_1 + h_2 + r{\cdot}h_2 - IA - q \bullet \theta_2 > w_{max}$$

$$Case\ 2 : h_1 + r{\cdot}h_1 - IA - q \bullet \theta_1 \le w_{max}; h_1 + r{\cdot}h_1 - IA - q \bullet \theta_1 - q \bullet d_1 \le 0; h_2 + r{\cdot}h_2 - IA - q \bullet \theta_2 > w_{max}$$

$$Case\ 3 : h_1 + r{\cdot}h_1 - IA - q \bullet \theta_1 > w_{max}; w_{max} - q \bullet d_1 \le 0; h_2 + r{\cdot}h_2 - IA - q \bullet \theta_2 > w_{max}$$

$$Case\ 4 : h_1 + r{\cdot}h_1 - IA - q \bullet \theta_1 > w_{max}; w_{max} - q \bullet d_1 > 0; w_{max} - q \bullet d_1 + h_2 + r{\cdot}h_2 - IA - q \bullet \theta_2 > w_{max}$$

In the following, it has been assumed that $h = h_1 = h_2$, $\theta = \theta_1 = \theta_2$, $d = d_1$.

Rearranging the conditions expressed by *Case* 1 and assuming it results:

$$h \le \frac{IA + q \bullet \theta + w_{max}}{1+r}; h > \frac{IA + q \bullet \theta + q \bullet d}{1+r}; h > \frac{q \bullet d}{2 \bullet (1+r)} + IA + q \bullet \theta + w_{max}$$

Rearranging the conditions expressed by *Case* 2 and assuming it results:

$$h \le \frac{IA + q \bullet \theta + w_{max}}{1+r}; h \le \frac{IA + q \bullet \theta + q \bullet d}{1+r}; h > \frac{IA + q \bullet \theta + w_{max}}{1+r}$$

Rearranging the conditions expressed by *Case* 3 and assuming it results:

$$h > \frac{IA + q \bullet \theta + w_{max}}{1+r}; d \ge \frac{w_{max}}{q};$$

Rearranging the conditions expressed by *Case* 4 and assuming it results:

$$h > \frac{IA + q \bullet \theta + w_{max}}{1+r}; d < \frac{w_{max}}{q}; h > \frac{q \bullet d + IA + q \bullet \theta}{2 \bullet (1+r)}.$$

The condition $v_2 > \bar{v}$ results:

$$h > \frac{q \bullet \theta + IA + w_{max} + \bar{v}}{1+r}; h > \frac{q \bullet \theta}{1+r} + \frac{w_{max} + IA + \bar{v} + q \bullet d}{2 \bullet (1+r)}; h < \frac{q \bullet \theta + w_{max} + IA}{1+r}; d < \frac{w_{max}}{q}.$$

The probability that runoff exceeds the selected threshold is:

$$P_{v2} = P(v > \bar{v}) = \int_{h=\frac{q\bullet\theta+IA+w_{max}+\bar{v}}{1+r}}^{\infty} f_h \bullet dh \bullet \int_{\theta=0}^{\infty} f_\theta \bullet d\theta +$$

$$+ \int_{h=\frac{q\bullet\theta}{1+r}+\frac{w_{max}+IA+\bar{v}+q\bullet d}{2\bullet(1+r)}}^{\frac{q\bullet\theta}{1+r}+\frac{w_{max}+IA}{(1+r)}} f_h \bullet dh \bullet \int_{d=IETD}^{\frac{w_{max}}{q}} f_d \bullet dd \bullet \int_{\theta=0}^{\infty} f_\theta \bullet d\theta =$$

$$= \gamma \bullet \left\{ (1-\beta_2^{'}) \bullet \left[e^{-\frac{\xi}{2\bullet(1+r)}\bullet(q\bullet IETD+\bar{v}} + w_{max} + IA) \right] + \beta_2^{'} \bullet e^{\psi \bullet IETD - (\bar{v}} + w_{max} + IA) \bullet \left(\frac{\psi}{q} + \frac{\xi}{1+r} \right) \right\}$$

with $\beta_2^{'} = \frac{\xi \bullet q}{q \bullet \xi + 2 \bullet \psi \bullet (1+r)}$.

The same procedure has been developed for $N > 2$.

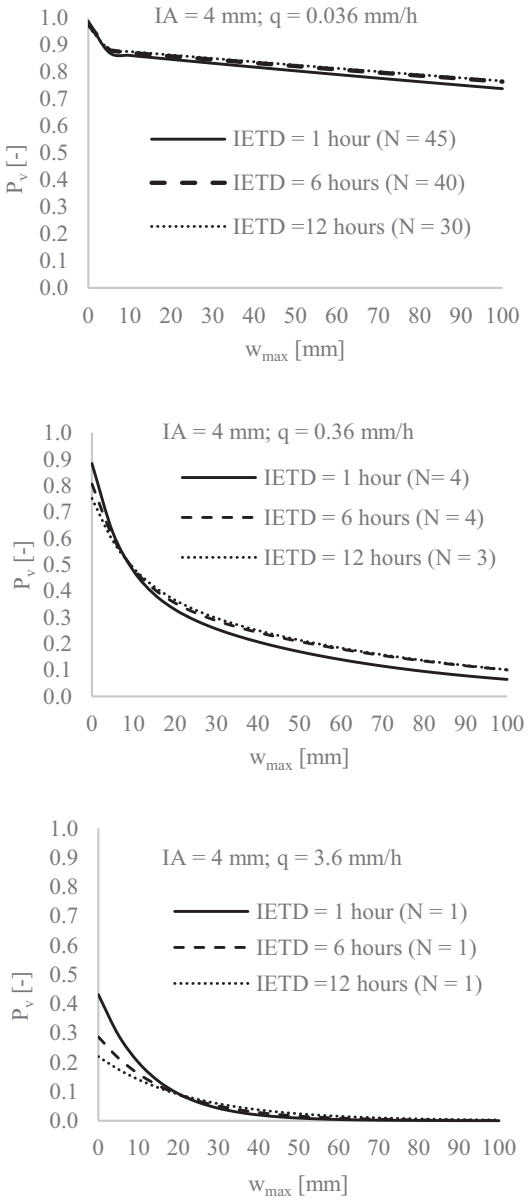

Fig. A1. Probability of runoff (P_v) varying the storage volume (w_{max}) for *IETD=1-6-12 h and q=0.036 mm/h (Fig. A1.1), q=0.36 mm/h (Fig. A1.2), and* q=3.6 mm/h (Fig. A1.3). IA=4 mm.

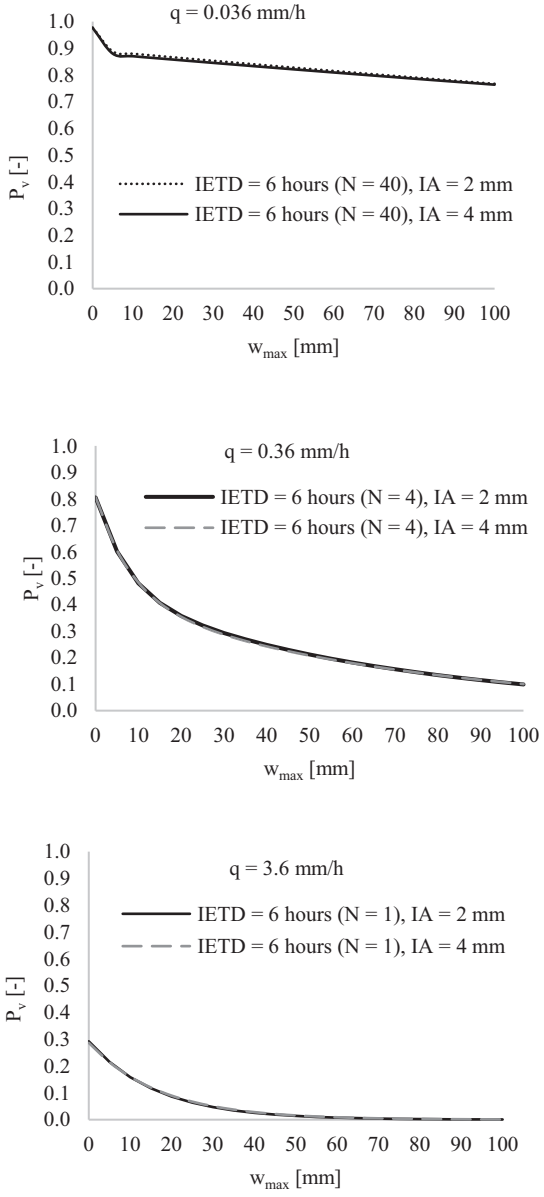

Fig. A2. Probability of runoff varying the retention volume (w_{max}) and IA, for q=0.036 mm/h (Fig. A2.1), q=0.36 mm/h (Fig. A2.2) and q=3.6 mm/h (Fig. A2.3). IETD=6 h.

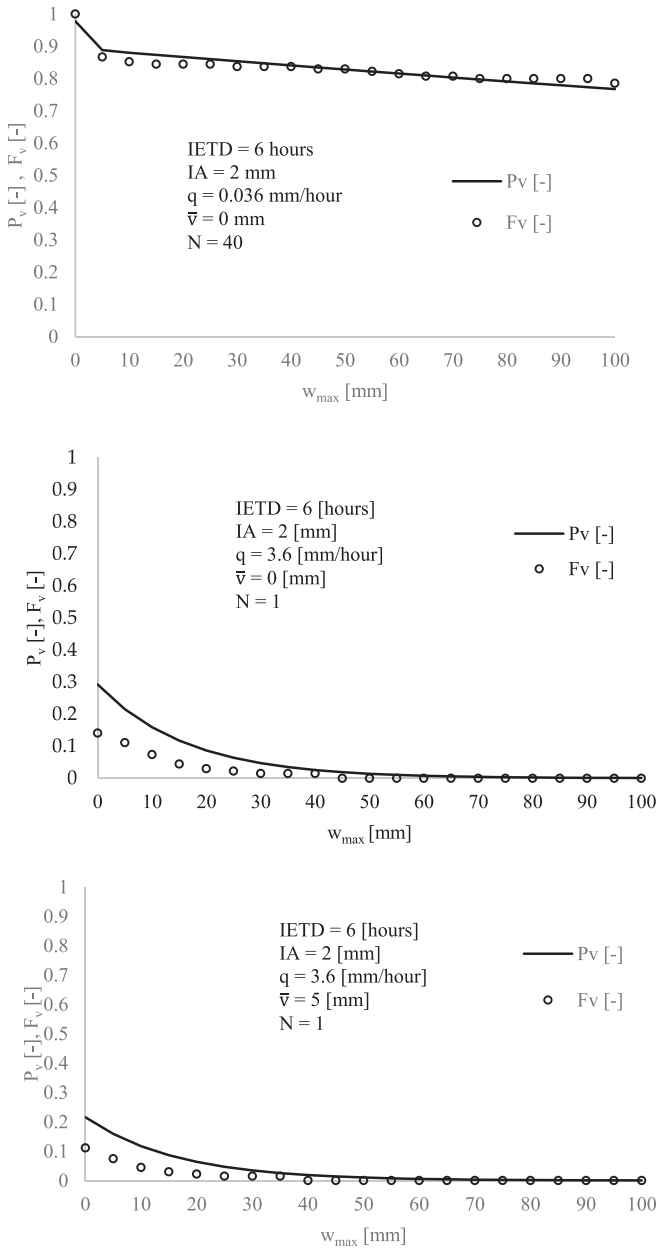

Fig. A3. Runoff probability (P_v) and frequency (F_v) varying the retention volume (w_{max}) considering two different runoff thresholds $\bar{v}$=0 mm and $\bar{v}$=5 mm (IETD = 6 h, q = 0.036 mm/h).

References

Adams, B.J., Papa, F., 2000. Urban Stormwater Management Planning with Analytical Probabilistic Models Wiley, New York, NY, 2000.

Aldrees, A., Danazumi, S., 2023. Application of analytical probabilistic models in urban runoff control systems' planning and design: a review. Water 15, 1640. https://doi.org/10.3390/w15091640.

Alivio, M.B., Bezak, N., 2023. Role of Trees as Part of the Nature-Based Solutions in Cities and Their Effects on Stormwater Runoff Generation. No. EGU23-3140. Copernicus Meetings.

Alsubih, M., Arthur, S., Wright, G., Allen, D., 2017. Experimental study on the hydrological performance of a permeable pavement. Urban Water J. 14 (4), 427–434. https://doi.org/10.1080/1573062X.2016.1176221.

Arjenaki, M.O., Sanayei, H.R.Z., Heidarzadeh, H., Mahabadi, N.A., 2021. Modeling and investigating the effect of the LID methods on collection network of urban runoff using the SWMM model (case study: Shahrekord City). Model. Earth Syst. Environ. 7 (1), 1–16. https://doi.org/10.1007/s40808-020-00870-2.

Balistrocchi, M., Bacchi, B., 2011. Modelling the statistical dependence of rainfall event variables through copula functions. Hydrol. Earth Syst. Sci. 15, 1959–1977. https://doi.org/10.5194/hess-15-1959-2011.

Barone, P.M., Ferreira, C., 2019. A posteriori GPR evaluation of tree stability a case study in Rome (Italy). Remote Sens. (Basel) 11, 1–17. https://doi.org/10.3390/rs11111301.

Bartens, J., Day, S.D., Harris, J.R., Dove, J.E., Wynn, T.M., 2008. Can urban tree roots improve infiltration through compacted subsoils for stormwater management? J. Environ. Qual. 37 (6), 2048–2057.

Becciu, G., Raimondi, A., 2012. Factors affecting the pre-filling probability of water storage tanks. WIT Trans. Ecol. Environ. 164, 473–484.

Becciu, G., Raimondi, A., Dresti, C., 2018. Semi-probabilistic design of rainwater tanks: a case study in northern Italy. Urban Water J. 15 (3), 192–199. https://doi.org/10.1080/1573062X.2016.1148177.

Berland, A., Shiflett, S.A., Shuster, W.D., Garmestani, A.S., Goddard, H.C., Herrmann, D. L., Hopton, M.E., 2017. The role of trees in urban stormwater management. Landsc. Urban Plan. 162, 167–177. https://doi.org/10.1016/j.landurbplan.2017.02.017.

Blunt, S.M., 2008. Trees and pavements —are they compatible? Arboricultural J. Int. J. Urban For. 31 (2) https://doi.org/10.1080/03071375.2008.9747522.

Brady, N.C., Weil, R.C., 2014. The Nature and Properties of Soil, 14th edition. Dorling Kindersley, India.

Campbell, L.K., 2014. Constructing new York City's urban forest: the politics and governance of the MillionTreesNYC campaign. In: Urban Forests, Trees, and Greenspace. Routledge, pp. 242–260.

Cao, S., Diao, Y., Wang, J., Liu, Y., Raimondi, A., Wang, J., 2023a. KDE-based rainfall event separation and characterization. Water 15 (3), 580.
Cao, S., Jia, J., Wang, J., Diao, Y., Liu, Y., Guo, Y., 2023b. Development of an analytical permeable pavement model for vehicular access areas. Sci. Total Environ. 883, 163686. https://doi.org/10.1016/j.scitotenv.2023.163686.
Chen, J., Barry, J.A., 2007. Development of analytical models for estimation of urban stormwater runoff. J. Hydrol. 336 (3–4), 458–469. https://doi.org/10.1016/j.jhydrol.2007.01.023.
Di Chiano, M.G., Marchioni, M., Raimondi, A., Sanfilippo, U., Becciu, G., 2023. Probabilistic approach to tank design in rainwater harvesting systems. Hydrology 10 (3), 59. https://doi.org/10.3390/hydrology10030059.
Eck, B.J., Barrett, M.E., Charbeneau, R.J., 2011. Coupled surface-subsurface model for simulating drainage from permeable friction course highways. J. Hydraul. Eng. 138 (1), 13–22. https://doi.org/10.1061/(ASCE)HY.1943-7900.0000474.
Fini, A., Frangi, P., Mori, J., Donzelli, D., Ferrini, F., 2017. Nature based solutions to mitigate soil sealing in urban areas: results from a 4-year study comparing permeable, porous, and impermeable pavements. Environ. Res. 156, 443–454. https://doi.org/10.1016/j.envres.2017.03.032.
Garofalo, G., Palermo, S., Principato, F., Theodosiou, T., Piro, P., 2016. The influence of hydrologic parameters on the hydraulic efficiency of an extensive green roof in Mediterranean area. Water 8, 44. https://doi.org/10.3390/w8020044.
Gasson, P.E., Cutler, D.F., 1990. Tree root plate morphology. Arboricult. J. 14, 193–264.
Gozzo, L.F., Palma, D.S., Custodio, M.S., Machado, J.P., 2019. Climatology and trend of severe drought events in the state of Sao Paulo, Brazil, during the 20th century. Atmosphere 10, 190. https://doi.org/10.3390/atmos10040190.
Guo, Y., Adams, B.J., 1998. Hydrologic analysis of urban catchments with event-based probabilistic models. I. Runoff volume. Water Resour. Res. 4 (12), 3421–3431.
Guo, R., Guo, Y., Wang, J., 2018. Stormwater capture and antecedent moisture characteristics of permeable pavements. Hydrol. Process. 32, 2708–2720. https://doi.org/10.1002/hyp.13213.
Huang, J., He, J., Valeo, C., Chu, A., 2015. Temporal evolution modeling of hydraulic and water quality performance of permeable pavements. J. Hydrol. 533, 15–27. https://doi.org/10.1016/j.jhydrol.2015.11.042.
Ishimatsu, K., Ito, K., Mitani, Y., Tanaka, Y., Sugahara, T., Naka, Y., 2017. Use of rain gardens for stormwater management in urban design and planning. Landsc. Ecol. Eng. 13 (1), 205–212. https://doi.org/10.1007/s11355-016-0309-3.
Jim, C.Y., 2017. Constraints to urban trees and their remedies in the built environment. In: Routledge Handbook of Urban Forestry. Routledge, pp. 273–290.
Johnson, T., City of Mitcham, 2015. Trees and permeable paving: future symbionts. In: TREENET Proceedings of the 16th National Street Tree Symposium.
Konijnendijk, C.C., Ricard, R.M., Kenney, A., Randrup, T.B., 2006. Defining urban forestry–a comparative perspective of North America and Europe. Urban For. Urban Green. 4 (3–4), 93–103. https://doi.org/10.1016/j.ufug.2005.11.003.
Kottek, M., Grieser, J., Beck, C., Rudolf, B., Rubel, F., 2006. World Map of the Köppen-Geiger Climate Classification Updated.
Lee, E.H., Kim, J.H., 2018. Development of new inter-event time definition technique in urban areas. KSCE J. Civ. Eng. 22, 3764–3771. https://doi.org/10.1007/s12205-018-1120-5.
Leming, M.L., Malcom, H.R., Tennis, P.D., 2007. Hydrologic Design of Pervious Concrete. Portland Cement Association, Skokie, IL.
Livesley, S.J., McPherson, E.G., Calfapietra, C., 2016. The urban forest and ecosystem services: impacts on urban water, heat, and pollution cycles at the tree, street, and city scale. J. Environ. Qual. 45 (1), 119–124. https://doi.org/10.2134/jeq2015.11.0567.
Lucke, T., Beecham, S., 2019. An infiltration approach to reducing pavement damage by street trees. Sci. Total Environ. 671, 94–100.
Lucke, T., Johnson, T., Beecham, S., Cameron, D.A., 2011. Using permeable pavements to promote street tree health, to minimize pavement damage and to reduce stormwater flows. In: 12th International Conference on Urban Drainage.
Madrazo-Uribeetxebarria, E., Garmendia Antín, M., Almandoz Berrondo, J., Andrés-Doménech, I., 2022. Modelling runoff from permeable pavements: a link to the curve number method. Water 15 (1), 160.
Marchioni, M., Raimondi, A., Andrés-Valeri, V.C., Becciu, G., Sansalone, J., 2021. Permeable pavement hydraulic conductivity indices for rainfall-runoff and particulate matter loadings. J. Environ. Eng. 147 (12), 04021064 https://doi.org/10.1061/(ASCE)EE.1943-7870.0001937.
Marchioni, M., Fedele, R., Raimondi, A., Sansalone, J., Becciu, G., 2022a. Permeable asphalt hydraulic conductivity and particulate matter separation with XRT. Water Resour. Manage. 36, 1879–1895. https://doi.org/10.1007/s11269-022-03113-4.
Marchioni, M., Raimondi, A., da Silva, J.C.D.A., de Lima Yazaki, L.F.O., Velasco, G.D.N., Sérgio, B., da Silva Filho, C.A., Becciu, G., 2022b. Soluções Baseadas na Natureza como instrumento de melhoria da arborização urbana, auxiliando na construção de cidades sensíveis à água e resilientes às mudanças climáticas. Revista LabVerde 12 (1), 12–44.
Medina Camarena, K.S., Wübbelmann, T., Förster, K., 2022. What Is the Contribution of Urban Trees to Mitigate Pluvial Flooding? Hydrology 9 (6), 108. https://doi.org/10.3390/hydrology9060108.
Morgenroth, J., Visser, R., 2011. Aboveground growth response of Platanus orientalis to porous pavements. Arboric. Urban For. 37 (1) https://doi.org/10.48044/jauf.2011.001.
Mullaney, J., Lucke, T., Trueman, S.J., 2015. The effect of permeable pavements with an underlying base layer on the growth and nutrient status of urban trees. Urban For. Urban Green. 14 (1), 19–29.
Muttuvelu, D.V., Kjems, E., 2021. A systematic review of permeable pavements and their unbound material properties in comparison to traditional subbase materials. Infrastructures 6 (12), 179. https://doi.org/10.3390/infrastructures6120179.
Nowak, D.J., Hirabayashi, S., Bodine, A., Greenfield, E., 2014. Tree and forest effects on air quality and human health in the United States. Environ. Pollut. 193, 119–129. https://doi.org/10.1016/j.envpol.2014.05.028.
Raimondi, A., Becciu, G., 2015. On pre-filling probability of flood control detention facilities. Urban Water J. 12 (4), 344–351. https://doi.org/10.1080/1573062X.2014.901398.
Raimondi, A., Becciu, G., 2021. Performance of green roofs for rainwater control. Water Resour. Manag. 35, 99–111. https://doi.org/10.1007/s11269-020-02712-3.
Raimondi, A., Marchioni, M., Sanfilippo, U., Becciu, G., 2021. Vegetation survival in green roofs without irrigation. Water 13 (2), 136. https://doi.org/10.3390/w13020136.
Raimondi, A., Di Chiano, M.G., Marchioni, M., Sanfilippo, U., Becciu, G., 2022. Probabilistic modeling of sustainable urban drainage systems. Urban Ecosyst. https://doi.org/10.1007/s11252-022-01299-4.
Raimondi, A., Sanfilippo, U., Marchioni, M., Di Chiano, M.G., Becciu, G., 2023. Influence of climatic parameters on the probabilistic design of green roofs. Sci. Total Environ. 865, 161291. https://doi.org/10.1016/j.scitotenv.2022.161291.
Rosa, A.S., Waetge, A.A.N., Barbosa, E.S., Biazzo, F.C.M., Kavamura, H.E., 2018. Diagnóstico das árvores caídas nos distritos da Subprefeitura Sé: análise de dados do período de 2016 A 2018, 2019. Trabalho de Conclusão de Curso, Especialização, Diadema: Universidade Federal de São Paulo, p. 42.
Ruangpan, L., Vojinovic, Z., Di Sabatino, S., Leo, L.S., Capobianco, V., Oen, A.M.P., McClain, M.E., Lopez-Gunn, E., 2020. Nature-based solutions for hydro-meteorological risk reduction: a state-of-the-art review of the research area. Nat. Hazards Earth Syst. Sci. 20, 243–270. https://doi.org/10.5194/nhess-20-243-2020.
Salvadori, G., De Michele, C., 2007. Frequency analysis via copulas: theoretical aspects and applications to hydrological events. Water Resour. Res. 40 (12) https://doi.org/10.1029/2004WR003133.
São Paulo (Cidade), 2015. Manual Técnico de Arborização Urbana. Secretaria Municipal do Verde e do Meio Ambiente. PMSP.
Schardong, A., Srivastav, R.K., 2014. Atualização da equação intensidade-duração-frequência para a cidade de são paulo sob efeito de mudanças climáticas. Rev. Bras. Recur. Hidr. 19 (4).
Scholz, M., Uzomah, V.C., 2013. Rapid decision support tool based on novel ecosystem service variables for retrofitting of permeable pavement systems in the presence of trees. Sci. Total Environ. 458, 486–498.
Smith, D.R., 2011. Permeable Interlocking Concrete Pavements, 4th ed. Interlocking Concrete Pavement Institute, Herndon, VA.
Terzaghi, K., Peck, R.B., Mesri, G., 1996. Soil Mechanics in Engineering Practice. John Wiley & Sons.
Tiwary, A., Sinnett, D., Peachey, C., Chalabi, Z., Vardoulakis, S., Fletcher, T., Hutchings, T.R., 2009. An integrated tool to assess the role of new planting in PM10 capture and the human health benefits: a case study in London. Environ. Pollut. 157 (10), 2645–2653.
Todeschini, S., Manenti, S., Creaco, E., 2019. Testing an innovative first flush identification methodology against field data from an Italian catchment. J. Environ. Manage. 246, 418–425.
Van Stan, J.T., Levia, D.F., Jenkins, R.B., 2015. Forest canopy interception loss across temporal scales: implications for urban greening initiatives. Prof. Geogr. 67 (1), 41–51. https://doi.org/10.1080/00330124.2014.888628.
Volder, A., Watson, T., Viswanathan, B., 2009. Potential use of pervious concrete for maintaining existing mature trees during and after urban development. Urban For. Urban Green. 8 (4), 249–256. https://doi.org/10.1016/j.ufug.2009.08.006.
Wang, J., Meng, Q., Zhang, L., Zhang, Y., He, B.J., Zheng, S., Santamouris, M., 2019. Impacts of the water absorption capability on the evaporative cooling effect of pervious paving materials. Build. Environ. 151, 187–197. https://doi.org/10.1016/j.buildenv.2019.01.033.
Weiss, P.T., Kayhanian, M., Gulliver, J.S., Khazanovich, L., 2019. Permeable pavement in northern North American urban areas: research review and knowledge gaps. Int. J. Pavement Eng. 20 (2), 143–162. https://doi.org/10.1080/10298436.2017.1279482.
Winston, R.J., Al-Rubaei, A.M., Blecken, G.T., Viklander, M., Hunt, W.F., 2016. Maintenance measures for preservation and recovery of permeable pavement surface infiltration rate–the effects of street sweeping, vacuum cleaning, high pressure washing, and milling. J. Environ. Manage. 169, 132–144. https://doi.org/10.1016/j.jenvman.2015.12.026.
World Meteorological Organization. State of the Global Climate, 2021. WMO Provisional Report. World Meteorological Organization, Geneva, Switzerland, p. 2021.
Xiao, Q., McPherson, E.G., Ustin, S.L., Grismer, M.E., 2000. A new approach to modeling tree rainfall interception. J. Geophys. Res. Atmos. 105 (D23), 29173–29188.
Xiao, Q., McPherson, E.G., 2016. Rainfall interception of three trees in Oakland, California. Urban Ecosyst. 14, 755–769. https://doi.org/10.1007/s11252-011-0192-5.
Yao, N., van den Bosch, C.C.K., Yang, J., Devisscher, T., Wirtz, Z., Jia, L., Ma, L., 2019. Beijing's 50 million new urban trees: strategic governance for large-scale urban afforestation. Urban For. Urban Green. 44, 126392. https://doi.org/10.1016/j.ufug.2019.126392.
Zhang, S., Guo, Y., 2013. Analytical probabilistic model for evaluating the hydrologic performance of green roofs. J. Hydrol. Eng. 18 (1) https://doi.org/10.1061/(ASCE)HE.1943-5584.0000593.
Zhang, S., Guo, Y., 2015. SWMM simulation of the storm water volume control performance of permeable pavement systems. J. Hydrol. Eng. 20 (8), 06014010 https://doi.org/10.1061/(ASCE)HE.1943-5584.0001092.
Zhang, L., Singh, V.P., 2007. Bivariate rainfall frequency distributions using Archimedean copulas. J. Hydrol. 332 (1–2) https://doi.org/10.1016/j.jhydrol.2006.06.033, 193-109.